05

Features of polymorphic transformation during heating and cooling of cobalt

© *L.V. Spivak,*[1] *N.E. Shchepina*[2]

[1] Perm State University,
Perm, Russia
[2] Institute of Natural Sciences of Perm State University,
Perm, Russia
e-mail: lspivak2@mail.ru, neshchepina@mail.ru

Received November 20, 2021
Revised January 3, 2022
Accepted January 24, 2022

Differential scanning calorimetry was used to study the regularities of polymorphic $\alpha \leftrightarrow \beta$-transformation in polycrystalline cobalt. The value of the activation energy of the $\alpha \to \beta$-transformation during heating of cobalt (290−50 kJ/mol), enthalpy and entropy, depending on the thermal history of the metal, is determined. It is shown that the mechanisms of recrystallization under heating are closer to the first-order I phase transformations. When cooling under conditions of limited diffusion mobility of cobalt atoms, recrystallization is apparently carried out due to the passage of several diffusion-free mechanisms of phase transformation, implemented in close temperature ranges.

Keywords: activation energy, cobalt, calorimetry, polymorphism, enthalpy, entropy.

DOI: 10.21883/TP.2022.04.53604.295-21

Introduction

It is believed that the mechanisms of polymorphic transformations in pure metals have already been characterized well both experimentally and theoretically (see [1–3]), and certain common features typical of this phenomenon have been formulated. As is often the case, the development of new and more sophisticated research techniques enables one to revisit the analysis of seemingly well-known axiomatics. This applies fully to the high-resolution differential scanning calorimetry (DSC) technique that was developed in recent years. However, having analyzed scientific literature published over the last 15 years, we found no reports made by other research groups that deal with DSC studies on polymorphism in such well-known metals as iron, titanium, zirconium, cobalt, and beryllium. A thorough DSC examination of polymorphic transformations in uranium [4] is somewhat of an exception to this. It turned out that $\alpha \to \beta \to \gamma$ transitions (rhombic → tetragonal → BCC lattice) occurring in the process of heating of uranium are governed by diffusion mechanisms, while mechanisms close to diffusion-free ones control the transitions during cooling. This rendition of mechanisms of direct and reverse polymorphic transformations in uranium is not entirely consistent with the current concepts. The results of DSC studies of polymorphic transformations in iron, zirconium, and titanium have been published relatively recently in [5–7]. It was demonstrated there that the common features of the $\alpha \leftrightarrow \gamma$ phase transformation are preserved in the polymorphic transformation in iron. However, the mechanisms of HCP ↔ BCC phase transitions in zirconium and titanium during heating differ from the mechanisms corresponding to cooling. The question of whether these features are also typical of HCP ↔ FCC polymorphic transformations has not been investigated to date. This is why the present study is focused on the examination of direct and reverse $\alpha \leftrightarrow \beta$ transformations in polycrystalline cobalt by DSC. There is all the more reason for this as, in regards to the HCP ↔ FCC polymorphic transformation in Co, the available data on temperatures of $\alpha \leftrightarrow \beta$ transformations (see, e.g., [8]), the magnitude of temperature hysteresis, and the enthalpy of such a phase transition are inconsistent.

1. Research procedure

Samples cut out from a 4-mm-thick plate of technically pure electrolytic cobalt (99.92% Co) were studied. DSC measurements were performed using a Jupiter 449 (Netzsch) simultaneous thermal analyzer. Heating and cooling were performed in argon (99.9995% Ar) atmosphere. The gas flow rate was 25−30 ml/min. The sample mass varied within the range of 180−210 mg. The experimental DSC data were processed using the Proteus thermal analysis software and the „Fityk“package. In order to exclude the possibility of emergence of artifacts related to the specifics of experimental examination of phase transformations, the obtained data were smoothed with a polynomial of order 6−8.

Each thermal cycle started from one and the same initial state of cobalt.

In the first scenario, this involved heating of a single sample at a rate of 40°C/min to 250°C and conditioning at this temperature for 5 min. After that, the same sample was subjected to a sequence of thermal cycles (250 ↔ 550°C) with heating and cooling rates of 5, 10, 20, and 40°C/min.

In the second scenario, a separate sample was used for each heating rate. These individual samples were heated to 250°C at a rate of 40°C/min, conditioned at this temperature for 5 min, and then heated or cooled at a rate of 5, 10, 20, or 40°C/min. The influence of the number of such thermal cycles (250 ↔ 550°C) on the thermodynamic parameters of polymorphic transformations was studied in the process.

2. Experimental results and discussion

In the first series of experiments, one and the same sample was successively heated and cooled at rates of 5−10−20−40°C/min. The results of one experiment of this kind are presented in Fig. 1.

Regardless of the thermal cycling pattern, the variation of the DSC signal under heating and cooling and the associated variation of the second derivative of this signal with respect to temperature (DDDSC) have certain common features. While the DDDSC maximum under heating is positioned within the temperature interval of the endothermic process, the curve of DDDSC variation under cooling has no minimum within the exothermic reaction interval. Hysteresis (70−80°C) between the onset temperature of transformation under heating and the onset temperature of transformation under cooling is evident. In addition, while the temperature of completion of the $\alpha \to \beta$ transition under heating may be identified reliably, the same temperature under cooling is not that well-defined.

The differences between $\alpha \leftrightarrow \beta$ transitions in Co under heating and cooling become evident if we present endothermic or exothermic maxima as a superposition of several subpeaks (Fig. 2).

The experimental data obtained during heating at moderate rates are approximated reasonably well by a single peak (Gaussian 1D), but the same is not true for cooling. Several subpeaks are required to approximate the exothermic maximum (Fig. 2, *b*). Apparently, this is indicative of the fact that two different mechanisms of nucleation of centers of the new phase with close activation temperatures are detected. A subpeak (P_3) reflecting the processes occurring throughout the entire temperature interval of phase transformation is present in all such cases.

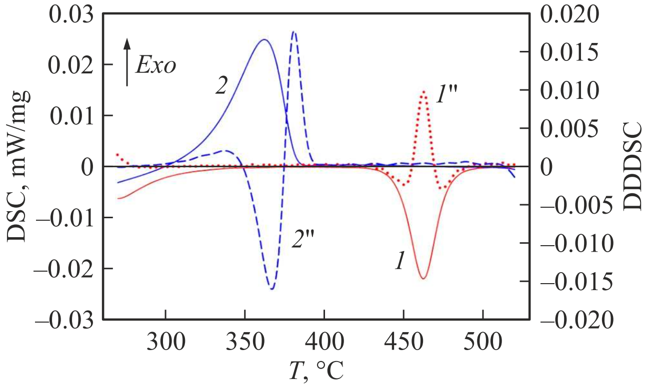

Figure 1. Variation of the DSC signal and its second derivative (DDDSC) under heating (*1*, *1''*) and cooling (*2*, *2''*) of Co at a rate of 5°C/min.

In the case of heating at rates in excess of 10°C/min, another subpeak (P_1) adjacent to the left front of the endothermic maximum is seen (Fig. 3, *a*) in approximation of the endothermic effect. The structure of the exothermic peak under cooling is preserved (Fig. 3, *b*).

These DSC dependences characterizing endothermic or exothermic effects may be attributed formally to a first-order phase transition (governed by a single mechanism of phase transformation) if the difference between the temperatures of the maximum (minimum) of the second derivative of the DSC signal with respect to temperature and the minimum (maximum) of the calorimetric effect is no greater than 0.1−0.3°C ([9,10]). Only the case of heating at a rate of 5°C/min satisfies this condition in our experiments. The mentioned temperature difference increases with the heating rate and reaches 2°C at 40°C/min. Figure 3, *a* illustrates this. The same applies in full to the results of approximation of exothermic maxima under cooling (Figs. 2, *b* and 3, *b*).

Figure 4, *a* shows the influence of the heating rate on the shape and positioning of endothermic peaks in the process of heating of cobalt in the first experimental scenario.

The so-called reduced specific heat capacity ($C_{p_{excess}}$ given by Eq. (1) (see [11]), where $\dot{Q}_S$ and $\dot{Q}_{Bl}$ are the heat fluxes in the process of heating with the sample and with base heat fluxes, respectively, m_s is the sample mass, and β is the heating rate [°C/s], is plotted on the ordinate.

$$C_{p_{excess}} = \frac{\dot{Q}_s - \dot{Q}_{Bl}}{m_s \beta}\,(\mathrm{Jg}^{-1}\cdot\mathrm{K}^{-1}). \qquad (1)$$

The curves presented in Fig.4, *a* are distinct in that the temperature of the endothermic peak minimum at a heating rate of 5°C/min is somewhat higher than the corresponding temperature under heating at a higher rate. For example, this temperature is 472.6°C at a heating rate of 5°C/min; 467.2°C at 10°C/min; 475.2°C at 20°C/min; and 488.8°C at 40°C/min. The thermal effect of transformation in this thermal cycling scenario depends only weakly on the heating rate and is equal to 3.4 ± 0.1 J/g. Thus, the effective enthalpy value is estimated at $\Delta H' = 0.20 \pm 0.01$ kJ/mol. This estimate is much lower than the enthalpy value obtained using the method of pulsed heating [12]: 0.45 ± 0.03 kJ/mol. Configuration entropy $\Delta S'$ falls within the range of 0.25−0.28 kJ/(mol · K) or $\Delta S' = 0.27 \pm 0.01$ J/(mol · K).

In the second experimental scenario, a new sample in the initial (as-fabricated) state was used for each heating rate. Each sample was subjected to three successive cycles of heating and cooling at a constant rate. The results of one experiment of this kind are presented in Fig. 5. It can be seen that the second and the third cycles yield close DSC

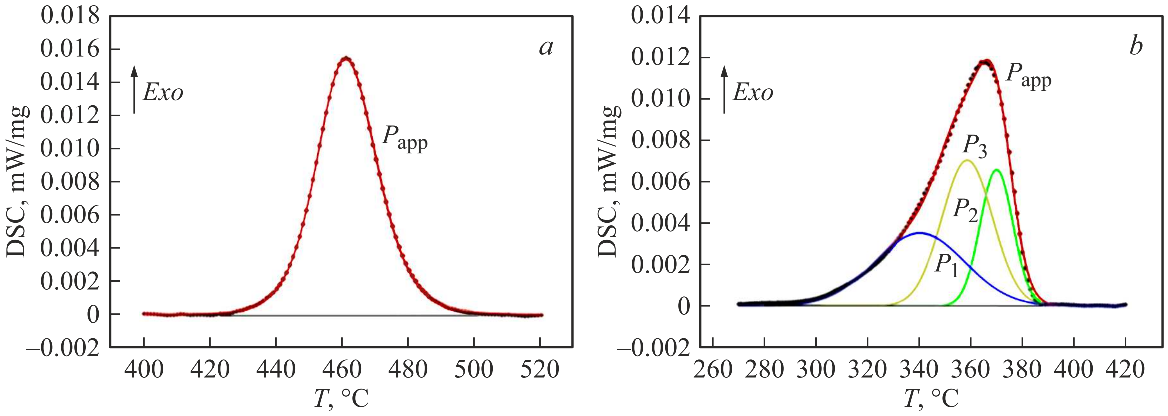

Figure 2. Structure of the endothermic peak under heating (*a*) and the exothermic peak under cooling (*b*) of cobalt. Points represent experimental data; P_{app} is the result of approximation; P_1, P_2, and P_3 are subpeaks. The thermal cycling rate is 5°C/min.

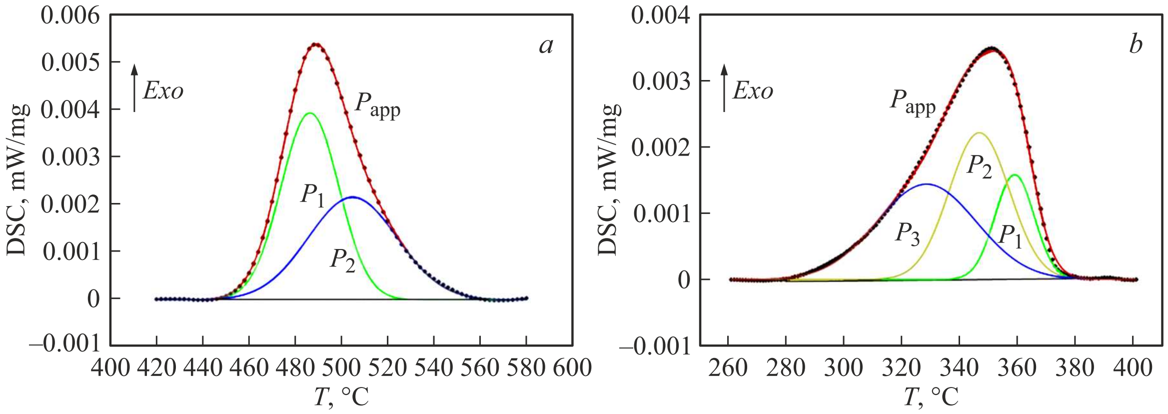

Figure 3. Structure of the endothermic peak under heating (*a*) and the exothermic peak under cooling (*b*) of cobalt. Points represent experimental data; P_{app} is the result of approximation; P_1, P_2, and P_3 are subpeaks. The thermal cycling rate is 40°C/min. Successive heating.

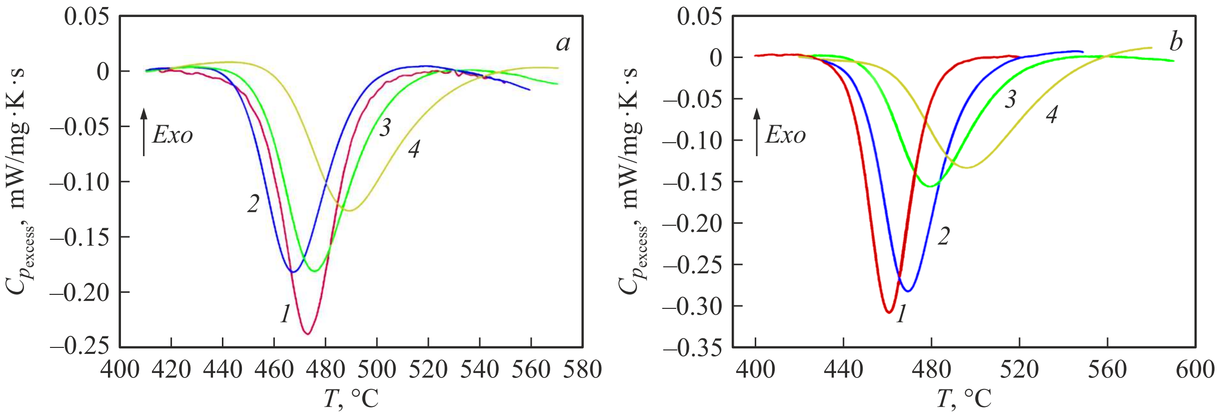

Figure 4. Influence of the heating rate on the shape and positioning of endothermic peaks in the $\alpha \rightarrow \beta$ transformation in Co. *1* — 5, *2* — 10, *3* — 20, *4* — 40°C/min; *a* — successive heating of one and the same sample; *b* — individual heating of samples (the second cycle).

signals measured in the process of heating, while the DSC minimum corresponding to the first cycle is positioned at higher temperatures. This is true for all heating rates.

As for the thermal effect of transformation, the following typical values averaged over three heating cycles correspond to different heating rates. At

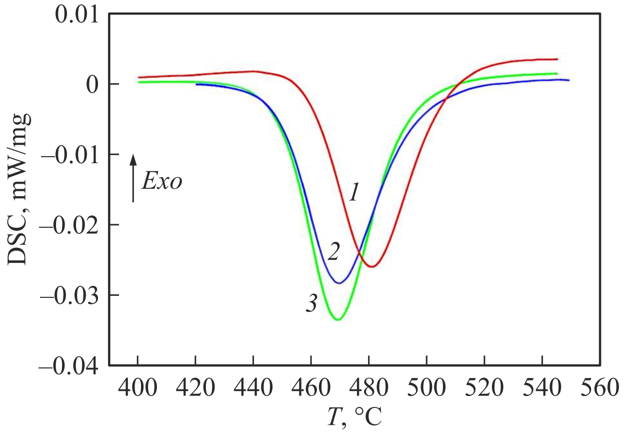

Figure 5. Influence of the number of heating cycles on the shape and positioning of the endothermic maximum in the $\alpha \to \beta$ transformation in Co. The heating rate is 10°C/min. *1* — first heating; *2* — second heating; *3* — third heating.

5°C/min: 5.3 ± 0.5 J/g; 10°C/min: 5.6 ± 0.3 J/g; 20°C/min: 4.0 ± 0.3 J/g; 40°C/min: 4.1 ± 0.3 J/g. The greatest thermal effect normally corresponds to the first heating.

Since the energy cost of the $\alpha \to \beta$ transition decreases is subsequent cycles, it appears logical to assume that a certain heritability mechanism, which reproduces to a certain extent the trajectory of displacement of atoms in the transition from the HCP structure to the FCC structure, is implemented here. This amounts to a certain element of memory, which was observed earlier in the successive thermal cycling scenario.

In the second experimental scenario, the influence of the heating rate on the structure of endothermic and exothermic minima and maxima is qualitatively similar to the one established in the case of successive heating of one and the same sample.

The influence of the heating rate on the DSC signal variation in the $\alpha \to \beta$ transition in Co in the second experimental scenario is presented in Fig. 4, *b*. Since the position of the maximum endothermic process rate shifts toward higher temperatures as the heating rate increases, one may estimate activation energy Q of the polymorphic transformation in Co in the $\alpha \to \beta$ transition using the Kissinger method [13]:

$$Q = -R\,\frac{\ln\left(\frac{\beta_1}{T_1^2}\right) - \ln\left(\frac{\beta_2}{T_2^2}\right)}{\left(\frac{1}{T_1} - \frac{1}{T_2}\right)}, \qquad (2)$$

where Q is the activation energy [kJ/mol]; R is the gas constant; T_1 and T_2 are the temperatures of maxima of the DSC signal dependence under heating; and β_1 and β_2 are the heating rates.

Ideally, the experimental points should form a single straight line when one plots the dependence of $\ln(\beta/T^2_{\max})$ on reciprocal temperature $1/T_{\max}$ of the endothermic maximum in the DSC signal curve. The slope of this curve provides an opportunity to estimate the activation energy of the $\alpha \to \beta$ transition. Figure 6, *a* presents the experimental results for the second heating cycle plotted in the indicated coordinates. It is evident that these data cannot be approximated by a single linear dependence. If one performs such an approximation, the method of solving of six pairwise Kissinger equations yields large errors in determination of the average value of Q (see earlier studies [6,7]).

Similar data for Ti [7] are shown in Fig. 6, *b* for comparison. The same is true for zirconium (see [6]).

Thus, the data in Fig. 6, *a* suggest that the activation energy of the polymorphic transformation in Co (Ti and Zr) depends on the heating rate. In the examined experimental scenario, an activation energy of 370−380 kJ/mol corresponds to low heating rates. The activation energy of the polymorphic transformation at higher rates is 230−240 kJ/mol. This is true for the first, the second, and the third cycles. Similar effects were observed in [14] for shape-memory alloys.

The dependence of the activation energy of the phase transition on the heating rate is likely attributable to a change in the mechanism of transition from one allotropic form of Co to the other. This correlates indirectly with the results of approximation of endothermic maxima by a single peak (low heating rate) or two subpeaks (high heating rates).

These data also attest to the trend that the energy cost of the $\alpha \to \beta$ transformation decreases as the heating rate increases.

Similar to the polymorphic $\alpha \to \gamma$ transformation in iron (see [5,6]), the $\alpha \to \beta$ transformation in Co at low heating rates proceeds primarily (see also [14]) in accordance with the diffusion-free mechanism (bulk transformation). The thermodynamic incentive for transformation and the diffusion mobility of Co atoms increase with the heating rate. This ensures the emergence and fairly rapid growth of new crystallites. As the heating rate increases, the differentiation of subpeaks in approximation of endothermic effects becomes more pronounced.

Since the difference in temperatures of the onset of transformation under heating and the onset of transformation under cooling is large (70−80°C) and the diffusion activity of Co atoms at moderate temperatures is relatively low, $\beta \to \alpha$ transformations under cooling (400−200°C) proceeds in accordance with different versions of the diffusion-free phase transition. The results of electron microscopic studies do indeed suggest the possibility of existence of three types of martensitic transformations in Co (see [15–19]): ε (HCP), ε' (4H or double HCP structure), and ε'' (9R or orthorhombic structure). Apparently, this is the reason why the exothermic process in this temperature region (Figs. 2, *b* and 3, *b*) is approximated by a superposition of three subpeaks. In the process of both heating and cooling, the subpeak covering the entire temperature range of observation of exo- or endothermic effects is likely attributable to the growth of emerging

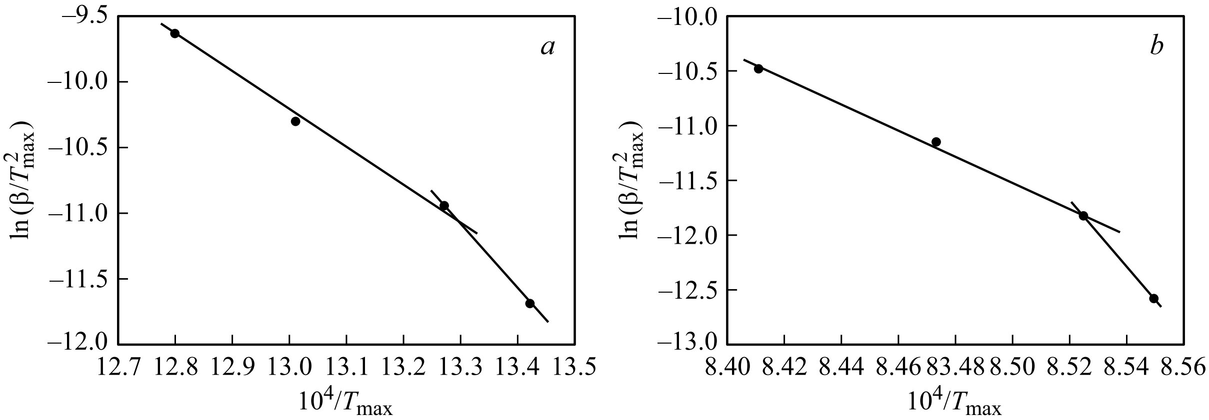

Figure 6. Dependence of $\ln(\beta/T_m^2)$ on the reciprocal temperature of the endothermic maximum in the process of heating of Co (a) and Ti (b) samples. Individual heating. The second cycle.

crystals of the new phase. The other subpeaks represent the process of emergence of new crystals.

It is instructive to compare the data for cobalt obtained in DSC studies with similar data for zirconium and titanium (see [6,7]). This comparison was performed for individual heating at a rate of 5°C/min, since this rate provides the closest approximation of a thermodynamic equilibrium state.

The thermal effect of the $\alpha \to \beta$ transformation for Co is 5.4 ± 0.2 J/g; the effective enthalpy value is $\Delta H' = 0.32$ kJ/mol, and the effective configuration entropy value is $\Delta S' = 0.43$ J/(mol · K).

The corresponding values for Ti are 40 ± 4 J/g; $\Delta H' = 1.9$ kJ/mol, $\Delta S' = 1.6$ J/(mol · K).

The corresponding values for Zr are 23 ± 2.6 J/g, $\Delta H' = 2.1$ kJ/mol, $\Delta S' = 1.8$ J/(mol · K).

It can be seen that the difference between metals with the HCP → BCC transition and HCP → FCC is fairly significant. Therefore, such a transition may be supported by different mechanisms.

The common patterns of the $\alpha \to \beta$ (HCP → BCC) transformation differ somewhat from those of the HCP → FCC transition. The most significant differences are as follows.

At all heating rates in Co, the DDDSC maximum falls within the temperature interval of observation of the endothermic effect. In zirconium an titanium, this is true only for heating rates in excess of 10°C/min.

No DDDSC maximum is observed for Co under cooling in the temperature range of the $\beta \to \alpha$ transformation. The exothermic effect may be represented as a superposition of three subpeaks.

In zirconium an titanium, this extremum of DDDSC curves emerges both under heating and under cooling at higher rates of thermal cycling. The exothermic effect under cooling is approximated well by two subpeaks (SplitGaussian).

Thermal cycling at a constant rate suppresses the thermal effect of the $\alpha \leftrightarrow \beta$ transformation in zirconium an titanium; in cobalt, this was not observed at all the studied rates of thermal cycling.

The temperature hysteresis between the onset of transformation under heating and the onset of transformation under cooling in cobalt is several times greater than the corresponding effect in zirconium an titanium. This last feature is an indirect indicator of the martensitic transformation mechanism.

Conclusion

The polymorphic $\alpha \leftrightarrow \beta$ transformation is manifested in Co under heating and cooling and proceeds in accordance with different mechanisms of atomic rearrangement. While this transformation under heating is close to a first-order phase transition (governed by a single mechanism of phase transformation), it turns into a superposition of calorimetric effects of several transformations, which occur in close temperature intervals, under cooling.

Polymorphic $\alpha \to \beta$ (HCP → BCC) transformations in Ti and Zr differ somewhat from the HCP → FCC transition in Co, and these differences cannot be reduced to just the variation of the spatial orientation of atoms (BCC or FCC). As was demonstrated above, they are related to the thermodynamic and kinetic features of this phase transformation.

The polymorphic transformation under heating of Ti, Zr, and Co is characterized by a dependence of the activation energy of this transition on the heating rate.

The behavior of studied metals with HCP lattices under heating and cooling within the temperature range of polymorphic transformation always depends to a certain extent on the thermal history of the specific sample under study.

Conflict of interest

The authors declare that they have no conflict of interest.

References

[1] Ya.S. Umanskii, Yu.A. Skakov. *Fizika metallov* (Atomizdat, M., 1978) (in Russian).

[2] R. Abbaschian, L. Abbaschian, R.E Reed-Hill. *Physical Metallurgy. Principles* (Cengage Learning ©, 2009)

[3] G.N. Haidemenopoulos. *Physical Metallurgy. Principles and Design* (CRC Press-Taylor and Francis 2018), DOI: 10.1201/9781315211220

[4] A.K. Rai, S. Raju, B. Jeyaganesh, E. Mohandas, R. Sudha, V. Ganesan. J. Nucl. Mater., **383**, 215 (2009).

[5] S.A. Oglezneva, L.V. Spivak, M.N. Kachenok, M.N. Portalov. Russ. Metall., **2015**, 250 (2015).

[6] L.V. Spivak, N.E. Shchepina. Tech. Phys., **65** (7), 1100 (2020). DOI: 10.21883/JTF.2020.07.49449.381-19

[7] L.V. Spivak, N.E. Shchepina. Tech. Phys., **66** (12), 1353 (2021). DOI: 10.21883/JTF.2021.08.51096.53-21s

[8] W. Betteridge. Progr. in Mater. Sci., **24**, 51 (1980).

[9] P.J. Van Ekeren. *Handbook of Thermal Analysis and Calorimetry Vol. 1: Principles and Practice,* M.E. Brown, editor. (Elsevier Science B., **75**, 1998)

[10] V.A. Aleshkevich. *Molekulyarnaya fizika* (Fizmatlit, M., 2016) (in Russian).

[11] S.M. Sarge, G.W.H. Höhne, W.F. Hemminger. *Calorimetry. Fundamentals Instrumentation and Applications* (Wiley-VCH Verlag GmbH & Co. KGaA: Weinheim, Germany, 2014)

[12] A.S. Dobrosavljevic, K.D. Maglic, N.L. Perovic. High Temp.-High Pressures, **21** (3), 317 (1989).

[13] H.E. Kisinger. Analyt. Chem., **29**, 1702 (1957).

[14] J.C. Zhao, M.R. Notis. Scripta Metall. Mater., **32** (10), 1671 (1995).

[15] Z.N. Zhou, L. Yang, R.C. Li, J.-G. Li. Intermetallics, **92**, 49 (2018).

[16] F. Cardellinia, G. Mazzonea. Phil. Mag. A., **67** (6), 1289 (1993).

[17] A. Muniera, J.E. Bidauxa, R. Schallera, C. Esnoufa. J. Mater. Res., **5** (4), 769 (1990).

[18] A.E. Ray, S.R. Smith. J. Phase Equilibria, **12** (6), 644 (1991).

[19] H. Matsumoto. J. Alloys Compounds, **223** (1), 11 (1995).